MAX-LOG-MAP SPHERE DECODER

Mong Suan Yee

Toshiba Research Europe Limited
32 Queen Square, Bristol, United Kingdom
Email: Mong.Yee@toshiba-trel.com

ABSTRACT

A max-log-MAP detector based on the sphere decoder is proposed and is shown to provide significant complexity reduction compared to the brute-force method for an equivalent channel coded BER performance. The algorithm is analysed for multiple antenna systems where the performance is compared to a list sphere decoder with bounded complexity for practical implementation.

1. INTRODUCTION

In receiver design for wireless communication, there is a need to develop efficient soft output detector algorithms for space time detection and multi-user detection, where error correction coding is utilized. Various near-optimal performance detectors have been proposed such as those based on sphere decoding, namely list sphere decoder (LSD) [1] and soft-to-hard sphere decoding [2]. The LSD involves searching for a list of possible transmitted symbols to derive the soft output in terms of *a posteriori* log likelihood ratio (LLR). The soft-to-hard sphere decoding proposed in [2] approximate the max-log-MAP (MLM) LLRs derivation based on the knowledge of the maximum likelihood (ML) transmitted bits. Sphere decoding is employed to obtain the maximum likelihood estimate and a set of candidates to derive the MLM LLRs is provided by 'bit-flipping' the found ML bit vector.

The LSD described in [1] suffers from the limitation that the sphere search radius cannot be reduced during the decoder search and the dependance of the soft output accuracy on the radius selected. For non-antipodal signalling such as quadrature amplitude modulation (QAM) scheme, the soft-to-hard sphere decoder requires the transformation of the QAM symbols to a linear combination of binary vectors, the use of prewhitening filter and employing bit-level multistream coded transmission [2]. To avoid the mentioned limitations, we follow the route of using multiple sphere decoders to provide the MLM LLR soft output.

The following section will describe the MLM decoding problem in the context of multiple-input/multiple-output (MIMO) system, followed by a brief introduction of sphere decoding technique. The concept of the proposed MLM sphere decoder is then introduced before a conclusion based on our simulation results.

2. CONCEPT

Consider the space time transmission scheme with $\tilde{n}_T$ transmitted and $\tilde{n}_R$ received signals, the $1 \times \tilde{n}_R$ received signal vector at each time instant is given by:

$$\tilde{\mathbf{r}} = \tilde{\mathbf{s}}\tilde{\mathbf{H}} + \tilde{\mathbf{v}}, \tag{1}$$

where $\tilde{\mathbf{s}} = [\ \tilde{s}^1 \quad \dots \quad \tilde{s}^{n_T}\ ]$ denotes the transmitted vector whose entries are chosen from a complex constellation $\tilde{C}$ with $\tilde{M} = 2^{\tilde{q}}$ possible signal points and $\tilde{q}$ is the number of bits per constellation symbol. The AWGN noise vector $\tilde{\mathbf{v}}$ is a $1 \times \tilde{n}_R$ vector of independent zero mean complex Gaussian noise entries with variance of σ^2 per real component. The notation $\tilde{\mathbf{H}}$ is the $\tilde{n}_T \times \tilde{n}_R$ MIMO channel matrix assumed to be known or estimated at the receiver, with n-row and m-column component $h_{n,m}, n = 1, \dots, \tilde{n}_T, m = 1, \dots, \tilde{n}_R$, representing the channel fading between the nth transmitted signal and mth received signal.

The complex matrix representation of Equation 1 can be transformed into the real matrix representation with twice the dimensions of the original system as follows:

$$\begin{aligned} \mathbf{r} &= \mathbf{s}\mathbf{H} + \mathbf{v}, && \text{where} \\ \mathbf{r} &= [\ \Re(\tilde{\mathbf{r}}) \quad \Im(\tilde{\mathbf{r}})\ ], \\ \mathbf{s} &= [\ \Re(\tilde{\mathbf{s}}) \quad \Im(\tilde{\mathbf{s}})\ ], \\ \mathbf{v} &= [\ \Re(\tilde{\mathbf{v}}) \quad \Im(\tilde{\mathbf{v}})\ ], \\ \mathrm{H} &= \begin{bmatrix} \Re(\tilde{\mathbf{H}}) & \Im(\tilde{\mathbf{H}}) \\ -\Im(\tilde{\mathbf{H}}) & \Re(\tilde{\mathbf{H}}) \end{bmatrix}. \end{aligned} \tag{2}$$

The following discussion uses the real-valued representation of Equation 2. For a square symbol constellations, each real component is chosen from the same real symbol constellation C with cardinality of $M = \sqrt{\tilde{M}}$ and $q = \tilde{q}/2$ number of bits per real symbol. The notation $n_T = 2\tilde{n}_T, n_R = 2\tilde{n}_R$ represents the number of real signal component transmitted and received, respectively.

The maximum *a posteriori* (MAP) probability bit detection of the jth bit of symbol s^n, x_j^n, conditioned on the received signal $\mathbf{r}$ can be expressed in LLRs as follows:

$$\begin{aligned} L_p(x_j^n|\mathbf{r}) &= \ln \frac{P(x_j^n = +1|\mathbf{r})}{P(x_j^n = -1|\mathbf{r})} \\ &= \ln \frac{\sum_{\mathbf{x} \in X_{n,j}^+} \exp(-\frac{\|\mathbf{r} - \hat{\mathbf{s}}\mathbf{H}\|^2}{2\sigma^2} + \frac{1}{2}\mathbf{x}^T\mathbf{L}_A)}{\sum_{\mathbf{x} \in X_{n,j}^-} \exp(-\frac{\|\mathbf{r} - \hat{\mathbf{s}}\mathbf{H}\|^2}{2\sigma^2} + \frac{1}{2}\mathbf{x}^T\mathbf{L}_A)} \\ & \qquad n = 1, \dots, n_T \qquad j = 1, \dots, q \end{aligned} \tag{3}$$

where $\mathbf{x} \in \{-1, +1\}^{n_T}$ is the sequence of possible transmitted bits, $\mathbf{L}_A$ is the vector of *a priori* LLR values of $\mathbf{x}$, $\hat{\mathbf{s}}$ is the vector of possible transmitted symbols, i.e. $\hat{\mathbf{s}} = \mathrm{map}(\mathbf{x})$, where the function map$(\cdot)$ provides the mapping from bits to symbol. The

The author would like to acknowledge the fruitful discussions with the collegues at Toshiba Research Europe and Toshiba Mobile Communication Laboratory Japan, and the support of its directors.

set $X_{n,j}^{+}$ and $X_{n,j}^{-}$ are the set of 2^{qn_T-1} bit vectors $\mathbf{x}$ having $x_j^n = +1$ and $x_j^n = -1$, respectively, i.e. $X_{n,j}^{+} = \{\mathbf{x}|x_j^n = +1\}$ and $X_{n,j}^{-} = \{\mathbf{x}|x_j^n = -1\}$.

The *a posteriori* LLR for each bit x_j^n defined in Eqn 3 can be approximated using the max-log approximation as follows:

$$L_P(x_j^n|\mathbf{r}) \approx \frac{1}{2}\max_{\mathbf{x}\in X_{n,j}^{+}}\left\{-\frac{\|\mathbf{r}-\hat{\mathbf{s}}\mathbf{H}\|^2}{\sigma^2}+\mathbf{x}^T\mathbf{L}_A\right\} - \frac{1}{2}\max_{\mathbf{x}\in X_{n,j}^{-}}\left\{-\frac{\|\mathbf{r}-\hat{\mathbf{s}}\mathbf{H}\|^2}{\sigma^2}+\mathbf{x}^T\mathbf{L}_A\right\} \quad (4)$$

Here, only the pair of candidates that provides the maximum of the term $-\frac{\|\mathbf{r}-\hat{\mathbf{s}}\mathbf{H}\|^2}{\sigma^2}+\mathbf{x}^T\mathbf{L}_A$ from the sets $X_{n,j}^{+}$ and $X_{n,j}^{-}$ is required to evaluate the MLM solution. The proposed MLM sphere decoder searches for this pair of candidates instead of evaluating for all 2^{qn_T} candidates. The next section will briefly describe sphere decoding before the full architecture of the MLM sphere decoder is presented.

3. SPHERE DECODER

The sphere decoder was introduced in [3] and has been applied to space time decoding in [4]. The principle of the algorithm is to search for candidate $\hat{\mathbf{s}}\mathbf{H}$ within a sphere of radius λ centered at the received signal $\mathbf{r}$, i.e.

$$\|\mathbf{r}-\hat{\mathbf{s}}\mathbf{H}\|^2 - \sigma^2\mathbf{x}^T\mathbf{L}_A \leq \lambda^2. \quad (5)$$

Each time a vector candidate $\hat{\mathbf{s}}$ is found, the search is restricted further by reducing the radius such that the found candidate is on the new search bound. There are three cases involved in the search algorithm [5], assumming the elements of $\hat{\mathbf{s}}$ are searched in the order of $\{\hat{s}^{n_T},\ldots,\hat{s}^1\}$:

- Case A: Each time the algorithm finds a point $\hat{s}^n$ inside the search bound during the nth level search, it expands its search to the $(n-1)$th symbol.
- Case B: A candidate $\hat{\mathbf{s}}$ is found if the search algorithm successfully found all valid points $\hat{s}_n, n = 1,\ldots,n_T$ inside the search bound.
- Case C: However, if the examined point is outside the search region, the algorithm moves up one step to examine the next candidate for the $(n+1)$th component of $\hat{\mathbf{s}}$.

The search algorithm can be seen as a tree search as shown in Figure 1 where every nth level node of the tree correspond to the search for the nth symbol of $\hat{\mathbf{s}}$. The search transverses down the tree and the branch of the tree is 'cut off' if the node gives an accumulated distance metric larger than the sphere radius. The number of nodes searched determines the complexity of the algorithm. For more information, Agrell et. al. [5] provides an informative semi-tutorial paper describing this search algorithm.

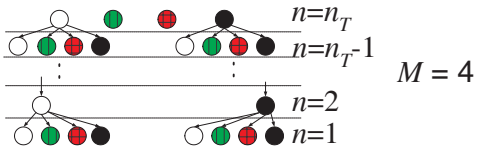

Fig. 1. Tree structure of the sphere decoder search algorithm.

Our paper uses the closest point search technique based on the Schnorr-Euchner strategy proposed in [5]. The search starts from the *Babai* point or the zero-forcing (ZF) solution $\mathbf{s}_{ZF} = (\mathbf{H}^T\mathbf{H})^{-1}\mathbf{H}^T\mathbf{r}$ and oscillates its search in turn from that point without explicitly deriving the upper and lower bound of the search region described in [6].

Reference [5] describes the search algorithm for the point $\hat{s}^n$ belonging to an infinite set of real integers. For the proposed MLM sphere decoder, the set of points to be searched, $\hat{s}^n$, is restricted to the finite symbol constellation with the jth bit x_j^n constrained to the value $+(-)1$, i.e. $\hat{s}^n = \text{map}(\mathbf{x}^n)$ where $\left[\begin{array}{ccc}\mathbf{x}^1 & \ldots & \mathbf{x}^{n_T}\end{array}\right] = \mathbf{x} \in X_{n,j}^{+(-)}$, as shown in Equation 4.

The search algorithm described by Agrell [5], where only one closest candidate is found, can be extended for 'list' sphere decoding [1]. LSD searches for a list of N_{cand} candidates $\hat{\mathbf{s}}\mathbf{H}$ nearest to the received signal $\mathbf{r}$ to provide a good approximation of Equation 3. Hence the list $\mathcal{L}$ contains the ML estimate and $N_{cand}-1$ neighbours. In [1], the sphere radius λ is kept constant and is chosen according to the channel statistic. We propose keeping the number of candidates in the list constant and reducing the sphere radius to the maximum distance metric found in the list, i.e, $\lambda = \max(d_1, d_2, \ldots, d_{N_{cand}})$ and d_i is the distance metrics of the ith candidate in the list. The sphere radius is initially set to a large value and is only reduced if the list is full. If a candidate is found inside the search region, the candidate with the maximum distance metrics in the list $\mathcal{L}$ is replaced by the new candidate and the sphere radius is updated. The soft ouput is evaluated according to Equation 4 but over the set $\mathbf{x} \in \mathcal{L} \cap X_{n,j}^{+}$ and $\mathbf{x} \in \mathcal{L} \cap X_{n,j}^{-}$. However, if there is no entry in the list with a prescribed bit value, i.e., $\mathcal{L} \cap X_{n,j}^{+(-)} = \varnothing$, the LLR value corresponding to bit x_j^n is set to an extreme LLR value $-x_{j,ML}^n|L|_{max}$, where $x_{j,ML}^n$ is the maximum likelihood estimate of bit x_j^n.

4. ARCHITECTURE

The pair of candidates, required to evaluate the LLRs as described in Equation 4, can be found from two stages of sphere decoding shown in Figure 2. For every received signal $\mathbf{r}$, the candidate with the shorter distance metrics among the pair found from set $X_{n,j}^{+}$ and $X_{n,j}^{-}$ for every bit in the sequence $\{x_j^n\}, n = 1,\ldots,n_T, j = 1,\ldots,q$, have the same minimum distance metrics d_{ML}^2 since one of the pair is the ML space time symbol estimate, $\mathbf{s}_{ML}$. The ML space time symbol is found by the sphere decoder at the first stage of the MLM sphere decoder architecture shown in Figure 2. Therefore, having known the ML bit sequence $\{x_{j,ML}^n\}$ corresponding to $\mathbf{s}_{ML}$, the derivation of $L(x_j^n|\mathbf{r})$, only requires the search of a candidate and its corresponding distance metrics $d_{n,j,-ML}^2$ from the set $X_{n,j}^{-ML}$ where the bit is reversed to that of the ML solution, i.e. $x_j^n = -x_{j,ML}^n$ and $s_{ML}^n = \text{map}(\mathbf{x}_{ML}^n)$. This is performed by the multiple sphere decoders at the second stage of the architecture shown in Figure 2.

4.1. Bounding Search Radius

The speed of the sphere decoder depends on the initial search radius. Setting the initial search radius to the distance metrics correspond to quantized $\mathbf{s}_{ZF}$ as described in [5] guarantees at least one candidate in the search region. Various techniques have been proposed to improve the search [7]. Here, we propose improving the search of the second stage sphere decoding with the information of

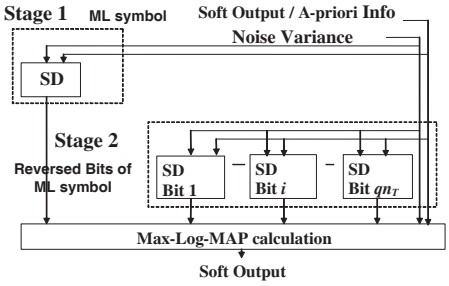

Fig. 2. Architecture of the MLM sphere decoder.

the lower distance metrics of the pair of candidate d_{ML} obtained at the first sphere decoding stage.

The initial search region of the second stage sphere decoding can be bounded according to the maximum LLR magnitude $|L|_{max}$ required by the application. Rewriting Equation 4, the MLM LLR is given by the pair of distance metrics $d_{n,j,+}$ and $d_{n,j,-}$ from the set $X_{n,j}^{+}$ and $X_{n,j}^{-}$, respectively, as follows:

$$L = \frac{1}{2\sigma^2}(-d_{n,j,+}^2 + d_{n,j,-}^2), \quad \text{giving} \tag{6}$$

$$|L| = \frac{1}{2\sigma^2}(d_{n,j,-ML}^2 - d_{n,j,ML}^2). \tag{7}$$

Therefore, the initial sphere radius of the second stage sphere decoding can be set as follows:

$$\lambda_{n,j,initial}^2 = d_{n,j,-ML}^2|_{|L|=|L|_{max}} = 2\sigma^2|L|_{max} + d_{ML}^2 \tag{8}$$

Note that the LLR magnitude $|L|$ indicates the reliability of the detection. Reference [8] demonstrates with a few channel decoders that a good extrinsic output gain is provided for low and medium *a priori* reliability but the output return diminishes for higher *a priori* reliability. Therefore, when the reliability of the detection or the a priori LLR magnitude is sufficiently high, there is little improvement to the channel decoding performance and it is reasonable to bound the LLR values provided to the channel decoder. The maximum LLR magnitude $|L|_{max}$ required which does not degrade the channel coded bit error rate (BER) performance will depend on the channel code and decoder used.

Assumming that the multiple sphere decoding in Figure 2 are performed sequentially, the candidates found during the previous sphere decoding $\{\hat{\mathbf{s}}_1, \hat{\mathbf{s}}_2, \ldots, \hat{\mathbf{s}}_P\}$, together with their corresponding distance metrics $\{d_1, d_2, \ldots, d_P\}$ is used as the initial estimate of $d_{n,j,-ML}$ at the current sphere decoding, i.e.

$$d_{n,j,-ML} = d_p \qquad \text{if } x_{j,p}^n = -x_{j,ML}^n \tag{9}$$

where $x_{j,p}^n$ is the jth bit for the nth symbol of the pth candidate found. These initial estimate is used to set the initial radius $\lambda_{n,j,initial}^2$ if it is lower than the bound set in Equation 8.

4.2. Bounded Complexity

The sphere decoder has variable complexity with the expected complexity studied in [9]. For practical implementation, the complexity of the sphere decoder has to be bounded where the node search is limited. The LLR is calculated according to Equation 6, based on the two distance metrics found after the limited tree node search. However, stopping the search, especially during the first stage where the ML symbol $\mathbf{s}_{ML}$ and distance metrics d_{ML} is estimated, will affect the accuracy of the derived LLRs passed to the channel decoder. This will degrade the channel coded BER performance as will be discussed in Section 5.

5. SIMULATION RESULTS

For the following simulations, a half-rate turbo coded, 4-by-4 (i.e. $\tilde{n}_T, \tilde{n}_R = 4$) 16QAM system is considered. A half-rate convolutional encoder with generator polynomial $(5, 7)_8$ is used in the turbo codec. The receiver is investigated over block invariant uncorrelated flat Rayleigh fading channel. We note that the MLM performance curve in all the figures is simulated with our proposed MLM sphere decoder with unbounded complexity. The notation E_b/N_o in the figures signifies the average signal energy to noise ratio per transmitted bit.

The effect of bounding the search radius as described in Section 4.1 is demonstrated in Figure 3. The turbo-coded BER performance shows little degradation from the MLM performance for $|L|_{max} \geq 4$.

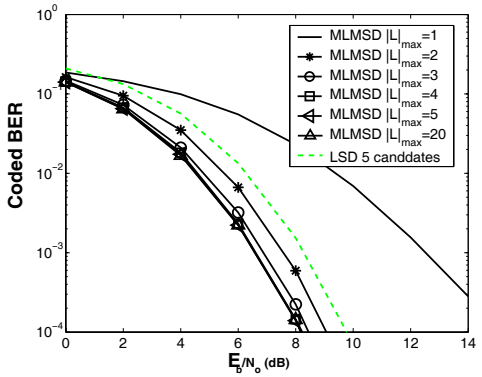

Fig. 3. BER performance of MLM sphere decoder with varying maximum LLR magnitude. The performance of the LSD with 5 candidates is shown for comparison.

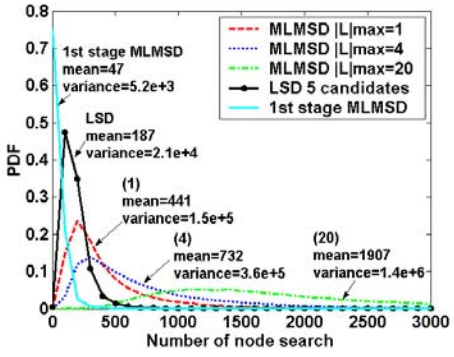

Fig. 4. Probability density function of the number of node search for MLM sphere decoder with varying maximum LLR magnitude, LSD and the first stage MLM sphere decoder at E_b/N_o = 8dB.

The probability density function (PDF) of the number of node

searches for the MLM sphere decoder with varying $|L|_{max}$ at E_b/N_o = 8dB is shown in Figure 4. The mean and variance of the PDF is given next to each curve. The PDF of node searches for the first stage sphere decoder which finds the ML space time symbol and for the LSD with five candidates are shown for comparison. Figure 4 shows a significant complexity reduction in terms of the number of node search by reducing the search radius for the sphere decoder in the second stage based on limiting the maximum LLR magnitude required. Note that the brute-force MLM space time decoder for 4-by-4 16QAM system will require $2 \times 4 \times 16^4 = 524288$ [1]. For example, the MLM sphere decoder with $|L|_{max} = 4$ will require 675 times less node searches on average compared to the full complexity MLM space time detector for an equivalent BER performance.

Figure 5 compares the BER performance with bounded complexity of n node search for list sphere decoder (LSDn) with five candidates and MLM sphere decoder (MLMSDn) with $|L|_{max}$ = 4. Since, the complexity of the LSD increases with increasing number of candidates required to evaluate the soft output, our simulation uses five candidates as a compromise between complexity and BER performance, where the LSD provides approximately 2dB performance degradation from the MLM performance as depicted in Figure 3. The performance gain for the MLM sphere decoder compare to the LSD is approximately 4dB, 6.5dB and 9dB for maximum node search of 1000, 500 and 200, respectively, at BER=10^{-4}. The performance gain is achieved by the MLM sphere decoder despite requiring a higher total number of unbounded node search compare to the LSD as shown in Figure 4. This performance gain is due to the faster sphere radius reduction for the first stage sphere decoder which searches for one candidate compare to the LSD with N_{cand} candidates to be considered as demostrated in Figure 4. Therefore, the probability that the ML symbol $\mathbf{s}_{ML}$ is found is lower for the LSD compare to the MLM sphere decoder for a limited number of search. The ML candidate determines the polarity of the LLR values and thus significantly affect performance of the channel decoder. The MLM sphere decoder with 1000 node search is approximately 1dB away from the MLM performance. The full complexity MLM detector for 4-by-4 16QAM system will require 524288 node searches. Therefore, the MLM sphere decoder with a maximum of 1000 node searches provide more than 500 times complexity reduction.

The BER performance of the minimum mean square error (MMSE) space time detector is provided in Figure 5 as a benchmark. Due to the inaccurracy of estimated LLR values when the complexity is bounded to 200 node search, the performance of the LSD is inferior compare to the MMSE detector. In order to speed up the search and to improve the bounded complexity performance, the MMSE solution can be used as the initial candidate.

6. DISCUSSION AND CONCLUSION

The proposed MLM detector based on sphere decoding has been analysed for MIMO system. The MLM sphere decoder provide a factor of 675 complexity reduction on average compare to the brute-force method for 4-by-4 16QAM system. For the same bounded complexity, the simulations show the MLM sphere decoder provide better performance compare to the LSD. The complexity of the sphere decoder can be further reduced by reordering the symbol detection as shown in [7, 10]. This will further improve the performance of the bounded complexity MLM sphere decoder.

[1] Two real component per complex symbol, four complex symbol per space time symbol and 16^4 possible candidates.

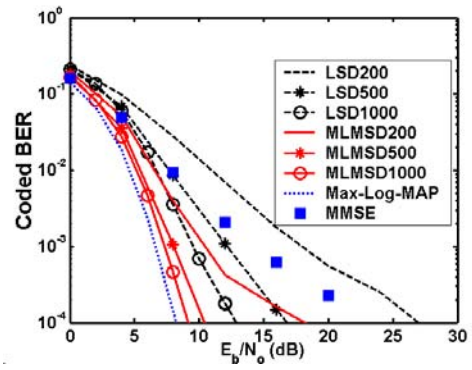

Fig. 5. BER performance comparison of MLM sphere decoder and LSD with bounded complexity. The performance of the MMSE space time decoder is shown as a benchmark.

7. REFERENCES

[1] B. M. Hochwald and S. T. Brink, "Achieving near-capacity on a multiple-antenna channel," *IEEE Trans. Commun.*, vol. 51, no. 3, pp. 389–399, Mar. 2003.

[2] R. Wang and G. B. Giannakis, "Approaching mimo channel capacity with reduced-complexity soft sphere decoding," in *Proc. Wireless Commun. and Networking Conf.*, Atlanta,USA, 21-24 Mar. 2004, pp. 1620–1625.

[3] U. Fincke and M. Pohst, "Improved methods for calculating vectors of short length in a lattice, including a complexity analysis," *Math. of Computation*, vol. 44, pp. 463–471, Apr 1985.

[4] O. Damen, A. Chkeif, and J. C. Belfiore, "Lattice code decoder for space-time codes," *IEEE Comms. Letter*, vol. 4, no. 5, pp. 161–163, May 2000.

[5] E. Agrell, T. Eriksson, A. Vardy, and K. Zeger, "Closest point search in lattices," *IEEE Trans. Inform. Theory*, vol. 48, no. 8, pp. 2201–2002, Aug. 2002.

[6] E. Viterbo and J. Boutros, "A universal lattice code decoder for fading channels," *IEEE Trans. Inform. Theory*, vol. 45, no. 5, pp. 1639–1642, Jul 1999.

[7] D. Pham, K. R. Pattipati, P. K. Willett, and J. Luo, "An improved complex sphere decoder for v-blast systems," *IEEE Sig. Proc. Lett.*, vol. 11, no. 9, pp. 748–751, Sept. 2004.

[8] S. T. Brink, "Convergence behavior of iteratively decoded parallel concatenated coded," *IEEE Trans. Commun.*, vol. 49, no. 10, pp. 1727–1737, Oct 2001.

[9] B. Hassibi and H. Vikalo, "On the expected complexity of sphere decoding," in *Conf. Record of the Thirty-Fifth Asimolar Conf. on Signals, Systems and Computers*, 2001, vol. 2, pp. 1051–1055.

[10] G. Caire M. O. Damen, H. E. Gamal, "On maximum-likelihood detection and the search for the closest lattice point," *IEEE Trans. Inform. Theory*, vol. 49, no. 10, pp. 2389–2402, Oct. 2003.